

UCRL- 94188  
PREPRINT

CIRCULATION COPY  
SUBJECT TO RECALL  
IN TWO WEEKS

THE EFFECT OF PARTIAL REVERSIBILITY  
OF DISLOCATION MOTION

A. W. Sleeswyk  
M. E. Kassner  
G. J. Kemerink

This paper was prepared for submittal to  
Symposium International sur les Deformations  
Finies des Agrégats: Bases Physiques et Modélisations,  
Paris, France, October 1985

January 17, 1986



Lawrence  
Livermore  
National  
Laboratory

This is a preprint of a paper intended for publication in a journal or proceedings. Since changes may be made before publication, this preprint is made available with the understanding that it will not be cited or reproduced without the permission of the author.

#### DISCLAIMER

This document was prepared as an account of work sponsored by an agency of the United States Government. Neither the United States Government nor the University of California nor any of their employees, makes any warranty, express or implied, or assumes any legal liability or responsibility for the accuracy, completeness, or usefulness of any information, apparatus, product, or process disclosed, or represents that its use would not infringe privately owned rights. Reference herein to any specific commercial product, process, or service by trade name, trademark, manufacturer, or otherwise, does not necessarily constitute or imply its endorsement, recommendation, or favoring by the United States Government or the University of California. The views and opinions of authors expressed herein do not necessarily state or reflect those of the United States Government or the University of California, and shall not be used for advertising or product endorsement purposes.

# THE EFFECT OF PARTIAL REVERSIBILITY OF DISLOCATION MOTION

A.W. Sleeswyk, M.E. Kassner\* and G.J. Kemerink

Lab. General Physics, University of Groningen,  
Westersingel 34, 9718 CM Groningen, The Netherlands

\*Lawrence Livermore National Laboratory,  
Livermore, California 94550, USA

## ABSTRACT

The partial reversibility of dislocation motion and strain hardening is studied by three different types of experiment.

1. It is shown that the Bauschinger effect in tension/compression tests must be explained by a 'lost strain' and an initial decrease in dislocation density when the mobile dislocations move between barriers after reversal. The model is confirmed by electron microscopy on the change of dislocation density after reversal.

2. Dislocations are made to move back and forth in a thin foil in the HVEM to which mutually perpendicular forces are applied alternately (x-y tests).

3. Mechanical analysis predicts that a large fraction of the mobile dislocations does not move when the tensile direction is changed over  $90^\circ$ . Macroscopic x-y tests on Al and Cu show that the strain hardening coefficient decreases after each change.

## RESUME

La réversibilité partielle du mouvement des dislocations et de l'écrouissage a été examinée par trois types d'expérience.

1. L'effet BAUSCHINGER observé dans des expériences du type traction/compression doit être expliqué par une 'traction perdue' et une diminution initiale de la densité des dislocations pendant le mouvement des dislocations mobiles entre barrières, après le renversement de la direction de la déformation. Le modèle est soutenu par des observations sur la densité des dislocations obtenues en microscopie électronique.

2. L'application alternante des forces de traction mutuellement perpendiculaires à une lame mince (expériences de traction x-y), permet de faire aller et venir les dislocations pendant observation dans un microscope électronique à haute tension.

3. Des expériences en traction x-y macroscopiques exécutées sur des échantillons d'aluminium et de cuivre font paraître une diminution importante du coefficient d'écrouissage après chaque changement x-y. D'autre part, une analyse mécanique prédit l'immobilité, après un changement x-y, d'une partie des dislocations d'abord mobiles.

## 1.- INTRODUCTION

The workhardening of a pure metal when the mechanical conditions are reversed is known in broad outline. The forces which propel mobile dislocations through the lattice change their signs, and many of the dislocations will, as a result, start to move in a direction opposite to the one they moved in previously.

Now, in general, tangles, braids or mats of dislocations will have been formed during the previous plastic straining. These constitute barriers to dislocation motion, causing strain hardening. They are mostly created from dislocations on intersecting planes gliding in opposite directions and trapping each other. Upon stress reversal, some of the trapped dislocations will escape from these barriers. The question is: what fraction of the trapped dislocations will escape, or: how stable are the barriers? What happens immediately after stress reversal?

It is of obvious interest to study the motion of a dislocation, and its subsequent reverse motion, in situ in the electron microscope. A difficulty in carrying out such an experiment is that it is virtually impossible to reverse mechanical conditions in a thin foil without causing it to buckle. We have developed a stratagem, which consists of changing the tensile direction over  $90^\circ$ . Mechanical analysis shows that under these conditions, many, but not all, mobile dislocations will reverse their paths. We have built and operated such an x-y tensile tester, and we have been able to make dislocations run back and forth in a foil while being observed in the electron microscope.

But if not all dislocations reverse their paths, it follows that trapping of dislocations on intersecting planes will happen less frequently. How are the yield stress and the strain hardening affected by alternate tensile tests in two mutually perpendicular directions? In order to answer this question, macroscopic tensile tests on sheet specimens must be performed, in which the tensile axis alternates between two mutually perpendicular directions. This kind of deformation occurs more frequently in forming processes of sheet material, i.e. pressing, deep drawing etc., than uni-axial tensile straining. The question has, in other words, its practical side. In the last section we describe experiments which throw light on it.

## 2.- THE BAUSCHINGER EFFECT IN TENSION/COMPRESSION TESTS

The starting point of our investigation of the Bauschinger effect in a pure stress reversal test was a discussion of the effect presented by Orowan in 1959. We carried out the experiments mainly with the aim of tracing the development of the effect during repeated forward and reverse plastic straining, as in low-cycle fatigue, Sleeswyk et al. (1978), James and Sleeswyk, (1978). In the present context the discussion is limited nearly exclusively to the first reversal.

Orowan discussed the phenomenology of the effect using the stress-strain diagram which is reproduced here in Fig. 1a. The forward strain hardening curve is OA. If the load is reduced to zero (B), the further plastic response of the material to mechanical loading is highly a-symmetric. If the plastic straining is continued in the forward sense, the resulting stress-strain curve is given by BAC, except for a small transient near A. Continuation of the plastic straining in the reverse sense results in a curve such as BD', or, if absolute stresses are plotted, BD. Orowan remarks that the curve BD is parallel to BAC, except for an initial transient. The difference in stress between the two curves is called the 'permanent softening', a concept introduced by Edwards and Washburn (1954).

Orowan remarked that back stresses, i.e. internal stresses exerted by dislocation configurations, "as rule are not the main factor in strain hardening", and that, although "a permanent softening has in fact been observed, ... its magnitude indicates that the back-stress effect is relatively small". Moreover, he remarked that the forward strain hardening curve OAC can be brought to near-coincidence with the reverse curve BD if it is shifted strain-wise over OE. Consequently "the material shows a permanent softening due to reversal, as if a part OE of the total plastic strain had been undone as far as its hardening effect is concerned".

What, then, is the physical cause of the Bauschinger effect? Is part of the plastic strain undone upon reversal, or is the back stress effect sufficiently large to cause permanent softening?

Wilson (1955) determined the magnitude of the internal stresses after plastic straining of aluminium alloy specimens by means of an X-ray method, and concluded

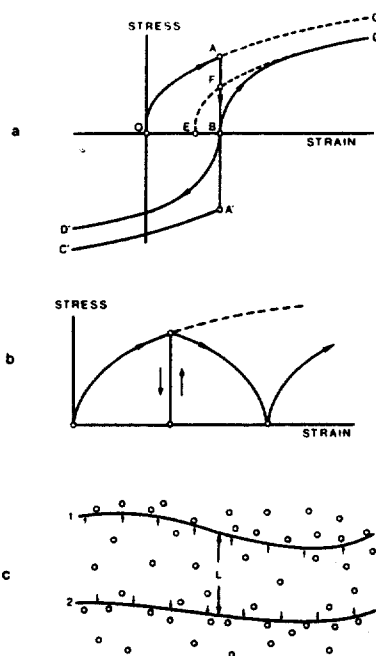


Fig. 1. a: Phenomenology of Bauschinger effect (Orowan, 1959);  
b: Taylor model solid under reverse straining; c: Dislocation  
mean free path  $L$  between barriers.

that the internal stresses are the cause of the permanent softening. Atkinson et al. (1973) used Wilson's result as a 'calibration' of their mechanical analysis, but they later pointed out (1975) that the method cannot be applied to pure materials.

There are reasons, however, for being skeptical about the proposed causal relationship. Permanent softening describes a stress bias of the whole specimen, while the internal stress, measured locally, is necessarily balanced by stresses of opposite sign elsewhere. In addition, that stress bias appears to persist indefinitely after reversal, while, on the other hand, it is perfectly clear from repeated reversals at various amplitudes that the stress bias caused by previous forward straining is replaced soon after reversal by one of opposite sign. The conclusion must be that the 'strain partially undone' - which we shall call 'lost' strain - is physically more significant than an apparent stress deficit.

Orowan briefly reviewed Taylor's (1934) model of strain hardening and the

reverse hardening curve - see Fig. 1b -, remarking that the latter is a highly unrealistic softening curve, then proceeded to explain the lost strain as an effect of the mean free path the mobile dislocations have to run through upon stress reversal. In the diagram (Fig. 1c) a dislocation is shown being pressed against a barrier consisting of obstacles under influence of the forward stress (position 1). When the reverse stress is applied, the mobile dislocations run through a trajectory of which the average length is  $L$  before coming to a halt again before a barrier (position 2). The magnitude of the lost strain  $\beta$  is  $\sim 0.02$ , and it is related to the mean free path  $L$  and the mobile dislocation density  $\rho_m$ :

$$\beta = \rho_m \cdot L \cdot b \quad (1)$$

in which  $b$  is the Burgers scalar. With:  $\rho_m = 10^{10} \text{ cm}^{-2}$ ,  $b = 2.10^{-8} \text{ cm}$ ,  $\beta = 0.02$ ,  $L$  must be  $10^{-4} \text{ cm}$ , 'a reasonable magnitude'.

The model was brought one step further by Sleeswyk et al. (1978), who remarked that the strain hardening curve represents barrier strength only if the mobile dislocations are being pressed against and passing these barriers. Evidently, that is not the case in the lost strain range  $\beta$  immediately after reversal. In addition, the barriers are partly composed of mobile dislocations on other glide planes which escape, and they will initially soften upon reversal. The assumption was introduced that this initial barrier softening, which takes place as long as no dislocations pass the barriers under reverse straining, is presented by the Taylor model, which implies that the forward hardening curve is now followed in reverse. In that stage, the applied stress is less than the barrier strength: at the strain where the stress is equal to it, the equilibrium between applied stress and barrier strength is re-established, and the Taylor model ceases to be applicable. That strain is characterised by the condition that the absolute values of the reverse and forward stress,  $\sigma_b$ , are equal; it marks the end of the transitional lost strain range  $\beta$ .

This extension of the Orowan model has the advantage that it can be verified experimentally, as  $\beta$  and  $\sigma_b$  can be determined from the forward and reverse strain hardening curves. As an example we present here the results of two tests on speci-

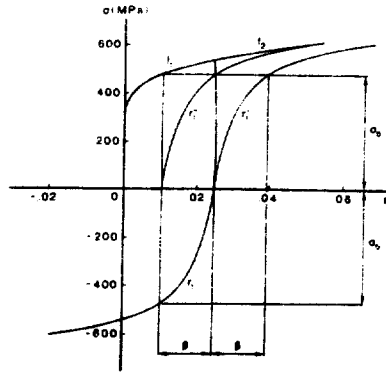


Fig. 2. Stress-strain curves obtained on annealed AISI 310; one tested forward and in reverse, the other tested monotonically.

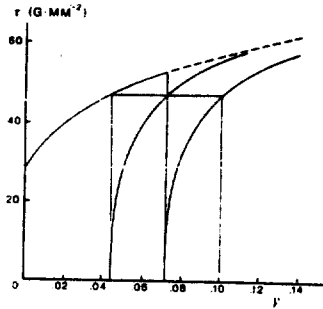


Fig. 3. Forward and reverse stress-strain curves obtained by Edwards and Washburn (1954) on a zinc single crystal.

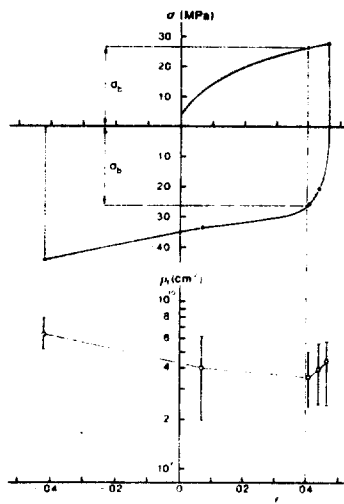


Fig. 4. Forward and reverse stress-strain curves and dislocation density - (reverse) strain curve obtained by Hasegawa et al. (1973) on aluminium.



mens of annealed AISI 310 stainless steel in the accompanying diagram (Fig. 2). One specimen was pulled to  $\sim 0.025$  plastic strain, at which point the straining was reversed, resulting in the forward and reverse hardening curves,  $f_1$  and  $r_1$ . If the latter is plotted in an absolute stress-strain diagram, the curve  $r_1'$  is obtained. That curve should be displaced towards the origin over  $\beta$  in order to account for the lost strain:  $r_1''$  results.

The second specimen was pulled monotonically, and the curve  $f_2$  resulted. It may be observed that the criterion not only gives a reasonable value of the lost strain  $\beta$  of  $\sim 0.0015$ , but that, in addition, the displaced reverse curve  $r_1''$  achieves coincidence with the forward curve  $f_2$  within a few percent strain after reversal.

We checked this effect on a number of specimens of aluminium, copper, nickel and stainless steel, and found it confirmed every time. The notion of permanent softening was supported by Edwards and Washburn (1954) by experimental results obtained on zinc single crystals. We have used the same data to determine  $\beta$ , and found that the displaced reverse curve approaches the extrapolated forward curve asymptotically, as required (Fig. 3).

Electron microscope observations of Hasegawa et al. (1975) on specimens of aluminium confirm that after stress reversal the dislocation density first decreases by about 16 %, then increases again. We have re-plotted their data in the diagram presented as Fig. 4. The vertical dashed line gives the critical value of  $\epsilon$  which limits  $\beta$ ; it may be observed that the decrease in dislocation density is limited to the  $\beta$  region. At any rate, these data provides a justification for the assumption that barrier softening takes place in this region, hence for the application of the Taylor model.

A further indication that the Taylor model provides a correct description of barrier softening in the  $\beta$ -region is the observation that  $\sigma_b$  is a constant fraction of the stress reached during the forward straining at reversal,  $\sigma_r$ . The value of this fraction  $\sigma_b/\sigma_r$  was found to be:  $\sigma_b/\sigma_r = 0.935$  for copper, aluminium and nickel, Sleeswyk (1985). It is independent of the values of stress and strain at reversal. The proportionality between  $\sigma_b$  and  $\sigma_r$  is illustrated in the diagram (Fig. 5). It may

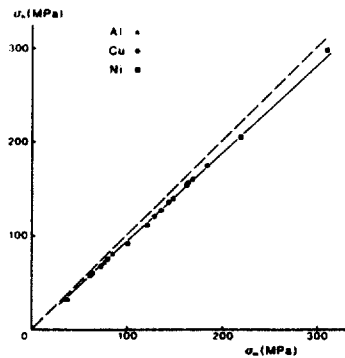


Fig. 5. Critical stress  $\sigma_b$  as a function of the stress  $\sigma_m$  at which the strain rate was reversed.

be added that no other pair of variables showed comparable correlation.

The Taylor model as applied to the non-equilibrium range  $\beta$  furnishes a ready explanation of the finding. It gives the following relation between the total dislocation density  $\rho_t$  and the applied stress:

$$\sigma = c \cdot \rho_t^{1/2}, \quad (2)$$

in which  $c$  is a constant.

The finding then implies that the ratio between dislocation densities at the end of the non-equilibrium range  $\beta$ ,  $\rho_b$ , and at reversal,  $\rho_r$ , should be  $(0.935)^2$ . It implies a maximum decrease of 12 %, which compares well with the 16 % decrease observed by Hasegawa et al. (see Fig. 4).

### 3.- IN SITU X-Y TENSILE TESTS IN THE ELECTRON MICROSCOPE

Tensile tests with stress axes at  $90^\circ$  to each other provide a possibility of reversing the velocities of mobile dislocations in thin foils. Although it appears feasible to perform reverse shear tests and even tension-compression tests on thin foils, Kubin and Lépinoux (1984), mechanical stability is an unsurmountable problem under these conditions. Buckling will inevitably occur, although in the electron microscope, with its enormous depth of field, this may manifest itself only as an inhomogeneity in mechanical conditions, which may escape attention. In order to

circumvent the problems associated with mechanical instability, we performed x-y tests, i.e. successive tensile tests in two mutually perpendicular directions in the plane of the foil.

Plastic deformation is to a very good approximation volume-invariant, and, consequently, uni-axial plastic strain along a given stress axis causes a negative plastic strain of half the magnitude in any direction perpendicular to it. (The material is assumed to be isotropic, the strains are defined as natural strains). Alternate plastic tensile straining much resembles, therefore, alternate tension/compression testing.

For a given glide plane (gd) and glide direction (gd) the shear stress component  $\tau_1$  resulting from the application of an applied stress  $\sigma_1$  along the stress axis ( $sa_1$ ) is given by the Schmid relationship, which may conveniently be expressed in the form:

$$\tau_1/\sigma_1 = 1/2 \cdot \sin \alpha_1 \cdot \sin 2\lambda_1, \quad (3)$$

where  $\alpha_1$  is the angle between the plane containing ( $sa_1$ ) and (gd), and the glide plane (gp), and  $\lambda_1$  is the angle between ( $sa_1$ ) and (gd). (This expression may be derived easily from the more customary form in which it is usually presented, using the equality:  $\cos \phi_1 = \sin \alpha_1 \cdot \sin \lambda_1$ ).

If now the stress  $\sigma_2$  is applied in a direction ( $sa_2$ ) perpendicular to ( $sa_1$ ), an extra parameter must be introduced in order to describe the position of ( $sa_2$ ) in the plane perpendicular to ( $sa_1$ ). That parameter is defined as the angle  $\beta$  between the plane containing ( $sa_1$ ) and (gd) and the plane containing ( $sa_1$ ) and ( $sa_2$ ); see the accompanying diagram (Fig. 6). The shear stress component  $\tau_2$  along (gd) on (gp) is now given by the expression:

$$\tau_2/\sigma_2 = -(\sin 2\beta \cdot \sin \lambda_1 \cdot \cos \alpha_1 + \cos^2 \beta \cdot \sin 2\lambda_1 \cdot \sin \alpha_1). \quad (4)$$

This expression is represented graphically in four diagrams for the  $\alpha_1$ -values of 0, 30, 60, and 90° (Fig. 7). Of course, as follows from eq. (4), for  $\beta = 90^\circ$  the value of  $\tau_2/\sigma_2$  is always equal to zero. Important are the diagrams for the larger  $\alpha_1$

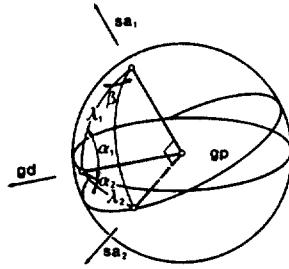


Fig. 6. Geometry of tensile tests along  $sa_1$  and  $sa_2$  in relation to a given glide plane (gp) and glide direction (gd).

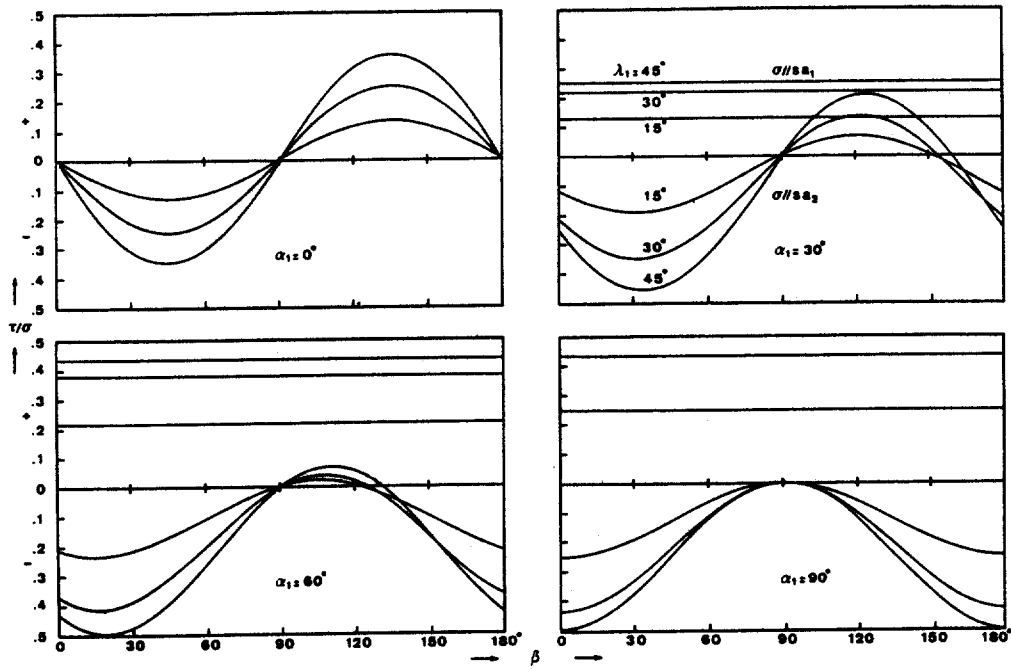


Fig. 7.  $\tau/\sigma$  vs.  $\beta$  diagrams for four  $\alpha$ -values, for both  $\tau_1/\sigma_1$  and  $\tau_2/\sigma_2$ .

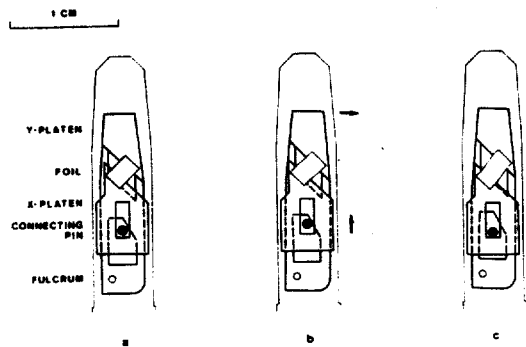


Fig. 8. a: Schematic of x-y tensile holder; b: y-platen activated by connecting pin; c: x-platen being pushed downwards.

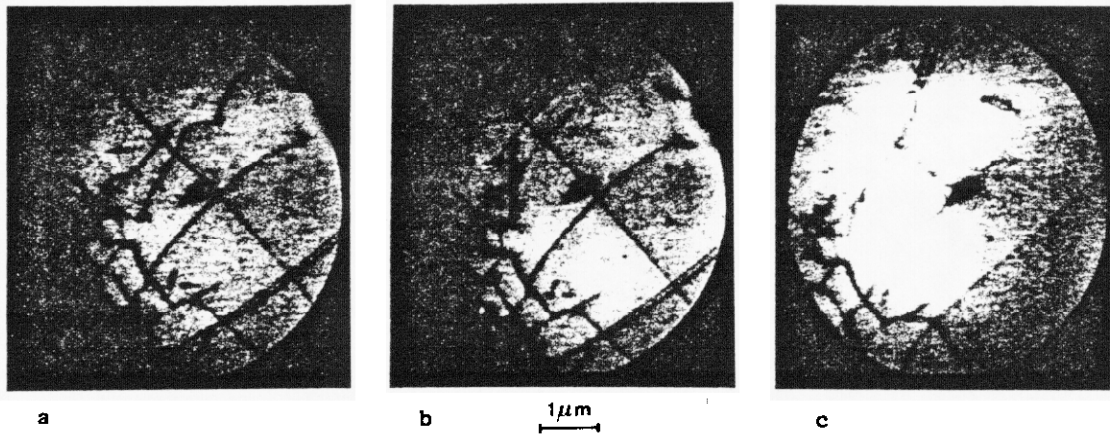


Fig. 9. Electron micrographs of dislocation configurations in aluminium. a: initial configuration; b: the same after tensile deformation in the x-direction; c: after an additional deformation in the y-direction.

values, where  $\tau_1/\sigma_1$  may reach values between  $\sim 0.2$  to  $0.5$ . For orientations with  $\beta$ -values close to  $0$  and  $180^\circ$  the values of  $\tau_2/\sigma_2$  are of the same magnitude as the  $\tau_1/\sigma_1$ -values, although of inverse sign. Only for  $\alpha_1 = 30^\circ$  do the diagrams show a region where the value of  $\tau_2/\sigma_2$  is of the same, rather low, magnitude, and the same sign. In general, dislocations that are mobile when  $\sigma_1$  is applied, will reverse their paths when  $\sigma_2$  is applied, or they will not move - e.g. when  $\beta$  is close to  $90^\circ$ .

In order to carry out the in situ x-y tests in the electron microscope, we designed and built a device in which the specimen is glued between two platens (Fig. 8). The lower one in the diagram can rotate around the fulcrum when the connecting pin, which is activated by an electric motor, moves upward, the upper one can slide down along the axis of rotation of the outer shell. The two platens are packed together in a slot in the outer shell of the holder. The top end of the lower platen is raised to the same level as the upper surface of the upper platen, in order to allow the foil to be mounted.

A few preliminary results are shown in the accompanying series of photomicrographs (Fig. 9). In Fig. a the initial dislocation configuration is shown, in Fig. b the dislocation configuration after application of a tensile load in the x-direction. A long dislocation in the upper half of the picture has glided in a SW direction, considerably shortening itself in the process, in the lower half some dislocations have annihilated themselves at the free surfaces of the foil. In Fig. 9c the dis-

locations are shown after application of a load in the y-direction. Now the dislocation in the upper half has elongated itself again, gliding NE. The long dislocation crossing through the middle of the picture has now partly annihilated itself. It seems it was prevented from doing so earlier because of the dislocation in the upper half being in the vicinity.

Except for the influence of the internal stresses exerted by other dislocations, the mobile dislocations generally behave as predicted by the equations (3) and (4).

#### 4.- MACROSCOPIC X-Y TENSILE TESTS

Alternate x-y tensile tests on thin plate specimens are interesting by themselves, because, as remarked earlier, in many forming processes of metal plate and sheet simultaneous or successive plastic tensile strains may occur in different directions. In addition, the equations (3) and (4) suggest that the similarity to tension/compression testing may not extend to the strain hardening process. In x-y tests only part of the mobile dislocations will move in the opposite direction after an x-y change, while in tension/compression tests all the forces on the dislocations are reversed and all mobile dislocations reverse their trajectories upon reversal. If strain hardening is due to dislocations on different glide planes trapping each other, one would expect that this would occur more often after strain rate reversal than after an x-y change.

Not much is known, however, about the effect of prior tensile testing along a different axis on anything but the yield locus, where it appears to be equivalent to that of a prior tensile deformation in the same direction.

We have carried out x-y tests on specimens machined from sheet material of a few mm thickness. The width was typically about 9 cm, while the distance between the jaws varied from 3 to 6 cm. As shown in the diagram (Fig. 10) the jaws are suspended alternately from positions located on the two stress axes passing through the centre of the specimen. No measurable effect is caused by the slight deviation from a right angle between the axes during the course of an experiment.

In the diagram presented as Fig. 11 the stress-strain curves obtained on

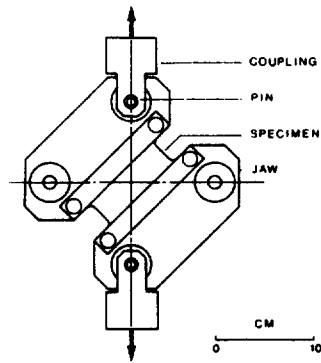


Fig. 10. Schematic of macroscopic x-y tensile testing jaws.

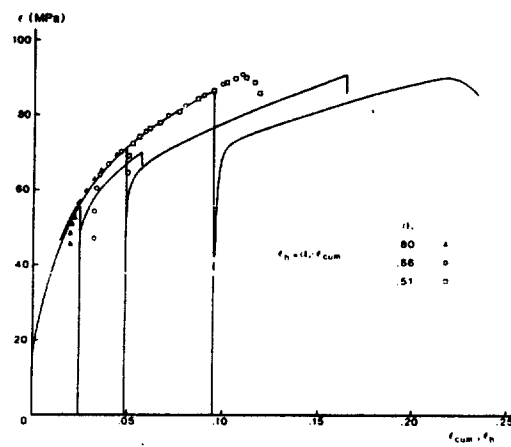


Fig. 11.  $\sigma$ - $\epsilon_{cum}$  curves obtained in x-y tests on three Al specimens. Points of the y-parts of the curves are plotted as  $\sigma$ - $\epsilon_h$ .

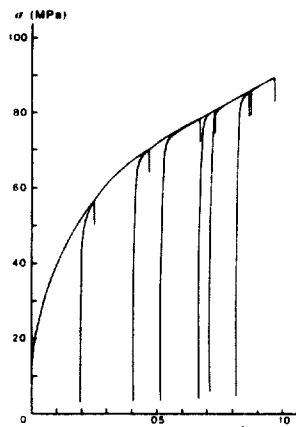


Fig. 12.  $\sigma$ - $\epsilon_h$  curves copied from plotter. These resulted from repeated x-y tests on one Al specimen. Adjustment of  $\alpha$  was performed by computer.

three specimens of polycrystalline aluminium of commercial purity are presented. These specimens had been vacuum-annealed at 520 °C, their gauge dimensions were: 29 x 89 x 2 mm. The x-plastic strain amplitudes chosen were: 0.024, 0.048 and 0.096. The two lower y-amplitudes were chosen such that the resulting cumulative strain would overlap the next-larger x-strain amplitude. At the largest amplitude the specimen was tested to incipient fracture.

It was noticed that the y-parts of the stress-cumulative strain curves largely coincided with the common x<sub>1</sub>-hardening curves if the cumulative strain values,  $\epsilon_{cum}$ , were each multiplied with a constant reducing factor  $\alpha_1$ , resulting in a homologous plastic strain  $\epsilon_h$ , or:

$$\epsilon_h = \alpha \cdot \epsilon_{cum} \quad (5)$$

This finding was illustrated in the diagram by plotting discrete points of the  $\sigma$ - $\epsilon_h$  curve for each of the specimens. Each of the specimens subjected to the x-y test has so far exhibited this remarkable behaviour. In addition to the specimens of commercial aluminium, a few of high purity (5N) metal were tested, and a few of copper.

As all our data are routinely stored on floppy disks, it was a relatively straightforward matter to devise a simple computerised fitting procedure for obtaining  $\alpha$ -values. The value of  $\alpha$  is required to be such that the stress vs. homologous strain curve passes through the end point of the previous curve. We made the computer plot the resulting stress vs. homologous strain curves: an example is the diagram reproduced as Fig. 12, which was copied from the computer plot. It gives the results of repeated x-y changes obtained on a single specimen. It may be observed that the  $\sigma$ - $\epsilon_h$  curve is an extrapolation of the first x-strain hardening curve, very much resembling the previous diagram obtained on a number of specimens. So far, we have not as yet observed counter examples, i.e. examples in which the  $\sigma$ - $\epsilon_h$  curve would not coincide with the  $\sigma$ - $\epsilon$  curve obtained in a monotonic tensile test.

The results obtained on three batches of aluminium specimens - two of commercial purity, one of 5N high-purity - are gathered in a  $\alpha$  vs.  $\epsilon_{cum}$  diagram (Fig. 13).



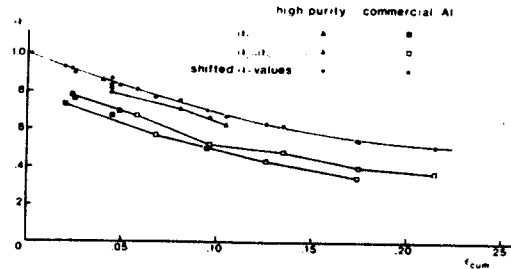


Fig. 13.  $\alpha$  plotted as a function of  $\epsilon_{cum}$  for three batches of aluminium. The results for different batches appear to differ only by a constant  $\alpha$ -value, as shown by the shifted data points.

The data points obtained by repeated x-y changes on a single specimen are interconnected by lines in order to distinguish them from  $\alpha_1$ -values. It seems that there is no obvious difference between  $\alpha_1$  and the other  $\alpha$ -values ( $\alpha_2 \dots \alpha_5$ ) within each batch of material. It appeared that the difference between the  $\alpha$ - $\epsilon_h$  curves for the three batches consisted of a difference in  $\alpha$ -level for each batch. We have illustrated this in the diagram by shifting the  $\alpha$ -values for each batch  $\alpha$ -wise, such that a single curve is defined by the data points. The finding implies that the initial  $\alpha$ -value, i.e.  $\alpha_1$ , is different for each batch.

The explanation of these effects can only be tentative, as electron microscope investigation of the specimens has only just started. It seems probable, however, that the difference between homologous and cumulative strain is caused by an increase in the mean free path of the dislocations after an x-y change. This would change the  $\epsilon$ -scale, the other parameters being unaffected. Why the initial  $\alpha$ -value is different for each batch of material can be due to a variety of causes: impurities, grain size differences, anisotropy or different initial dislocation configurations.

The finding that prior transverse tensile deformation affects the strain hardening coefficient has, of course, a bearing on the understanding of the formation of plastic instabilities during forming processes. It may be possible that the effect provides a method for ameliorating plastic stability during forming processes.

#### ACKNOWLEDGMENTS

Work performed under the auspices of the U.S. Department of Energy by the Lawrence Livermore National Laboratory under Contract W-7405-Eng-48.

## REFERENCES

- Atkinson, J.D., Brown, L.M. and Stobbs, W.M. (1973) "Recovery and the Bauschinger effect in Cu-SiO<sub>2</sub>", Proc. 3rd Conf. Strength Metals Alloys, Cambridge, 36.
- Atkinson, J.D., Brown, L.M. and Stobbs, W.M. (1975) "The work-hardening of copper-silica", Phil. Mag. 31, 1247.
- Edwards, E.H. and Washburn, J. (1954) "Strain Hardening of Latent Slip Systems in Zinc Crystals", Trans. AIME, 82, 1239.
- Hasegawa, T., Yakou, T. and Karashima, S. (1975) "Deformation Behaviour and Dislocation Structures upon Stress Reversal in Polycrystalline Aluminium", Mater. Sci. Eng. 20, 267.
- James, M.R. and Sleeswyk, A.W. (1978) "Influence of intrinsic stacking fault energy on cyclic hardening", Acta Met. 26, 1721.
- Kubin, L. and Lépinoux, J. (1984) "Développements récents sur les porte-objets pour microscopie électronique in situ", J. Microsc. Spectrosc. Electron. 9, 319.
- Orowan, E. (1959) "Causes and effects of internal stresses", Internal Stresses and Fatigue in Metals, G.M. Rassweiler and W.L. Grube (eds.), Elsevier Publ. Co., New York, 71.
- Sleeswyk, A.W., James, M.R., Plantinga, D.H. and Maathuis, W.S.T. (1978) "Reversible strain in cyclic plastic deformation", Acta Met. 26, 1265.
- Sleeswyk, A.W. and Kemerink, G.J. (1985) "Similarity of the Bauschinger effect in Cu, Al and Ni", Scripta Met. 19, 471.
- Taylor, G.I. (1934) "The mechanism of plastic deformation I", Proc. Roy. Soc. (London), A 145, 362.
- Wilson, D.V. (1965) "Reversible work hardening in alloys of cubic metals", Acta Met. 13, 807.